United States Department of Commerce
Technology Administration
National Institute of Standards and Technology

NISTIR 5073

Uncertainty Analysis Procedures for Dynamic Radar Cross Section Measurements at the Atlantic Test Range

J. Sorgnit
P. Mora
L.A. Muth
R.C. Wittmann

NISTIR 5073

Uncertainty Analysis Procedures for Dynamic Radar Cross Section Measurements at the Atlantic Test Range

J. Sorgnit
P. Mora
L.A. Muth
R.C. Wittmann

Electromagnetic Fields Division
Electronics and Electrical Engineering Laboratory
National Institute of Standards and Technology
Boulder, Colorado 80303-3328

February 1998

U.S. DEPARTMENT OF COMMERCE, William M. Daley, Secretary
TECHNOLOGY ADMINISTRATION, Gary R. Bachula, Acting Under Secretary for Technology
NATIONAL INSTITUTE OF STANDARDS AND TECHNOLOGY, Raymond G. Kammer, Director

Uncertainty Analysis Procedures for Dynamic Radar Cross Section Measurements at the Atlantic Test Range*

J. Sorgnit and P. Mora,[†]
L. A. Muth and R. C. Wittmann[‡]

National Institute of Standards and Technology
325 Broadway
Boulder, CO 80303-3328

February 11, 1998

Abstract

This report, which follows general guidelines proposed by the National Institute of Standards and Technology, documents uncertainty analysis procedures for radar cross section measurements as implemented at the Atlantic Test Range, Naval Air Warfare Center Aircraft Division at Patuxent River, MD. Example uncertainty computations are presented.

Key words: error budget; measurement uncertainties; radar cross section measurements; RCS; uncertainty analysis

---

*Distribution authorized to Department of Defense components and U.S. Department of Commerce only; Administrative or Operational Use; October 1995.

[†]NAWC-AD, Patuxent River, MD

[‡]NIST, Electromagnetic Fields Division, Boulder, CO

1 Introduction

In this report on radar cross section (RCS) measurement uncertainty, we follow the basic outline and format of Reference [1], wherein the National Institute of Standards and Technology (NIST) has proposed guidelines for estimating uncertainties in RCS measurements. It is our intent to list sources of RCS measurement errors at the Naval Air Warfare Center Aircraft Division (NAWC-AD), Patuxent River, MD RCS facility and to document procedures for estimating the corresponding uncertainties. Measurement uncertainty is dependent on the operational parameters of a dynamic RCS range. Typical operating conditions and parameters of dynamic range measurements (listed in Appendix A) are assumed for the analysis presented in this report; where appropriate, additional assumptions are stated explicitly.

The Atlantic Test Range (ATR) (shown in Figures 1 and 2) performs RCS measurements on in-flight aircraft for United States military and civilian customers. Located at Patuxent River, Maryland, at the mouth of the Patuxent River on Chesapeake Bay, the ATR is a part of the Atlantic Ranges and Facilities, a division of the Naval Air Warfare Center Aircraft Division.

The ATR currently operates *noncoherent* RCS systems capable of making simultaneous measurements in the D, E, G, H, I, J, and K bands (see Appendix A for system parameters). Typical measurements performed with these systems include: whole body RCS, chaff RCS, jammer-skin ratio (J/S), decoy-skin ratio (D/S), and antenna pattern measurements.

Additionally, the ATR is developing a coherent system to make simultaneous RCS measurements in the E, H, I, and J bands. This system will be able to measure Doppler signatures, and to produce 1D and 2D radar images.

STIPULATIONS AND INTERPRETATION—The following considerations apply:

1. This report identifies *procedures* that, if followed diligently, can lead to a defendable estimate of RCS measurement uncertainty.

2. Uncertainties must be determined for each RCS measurement. The values used in this report do not necessarily reflect a specific measurement, but are given for illustration.

3. Uncertainties in this report have been determined using NAWC-AD system parameters. The *values* of these parameters *have not been verified or endorsed by NIST*. These parameters are critical in determining

Figure 1: Aerial view of the Atlantic Test Range site at Patuxent River.

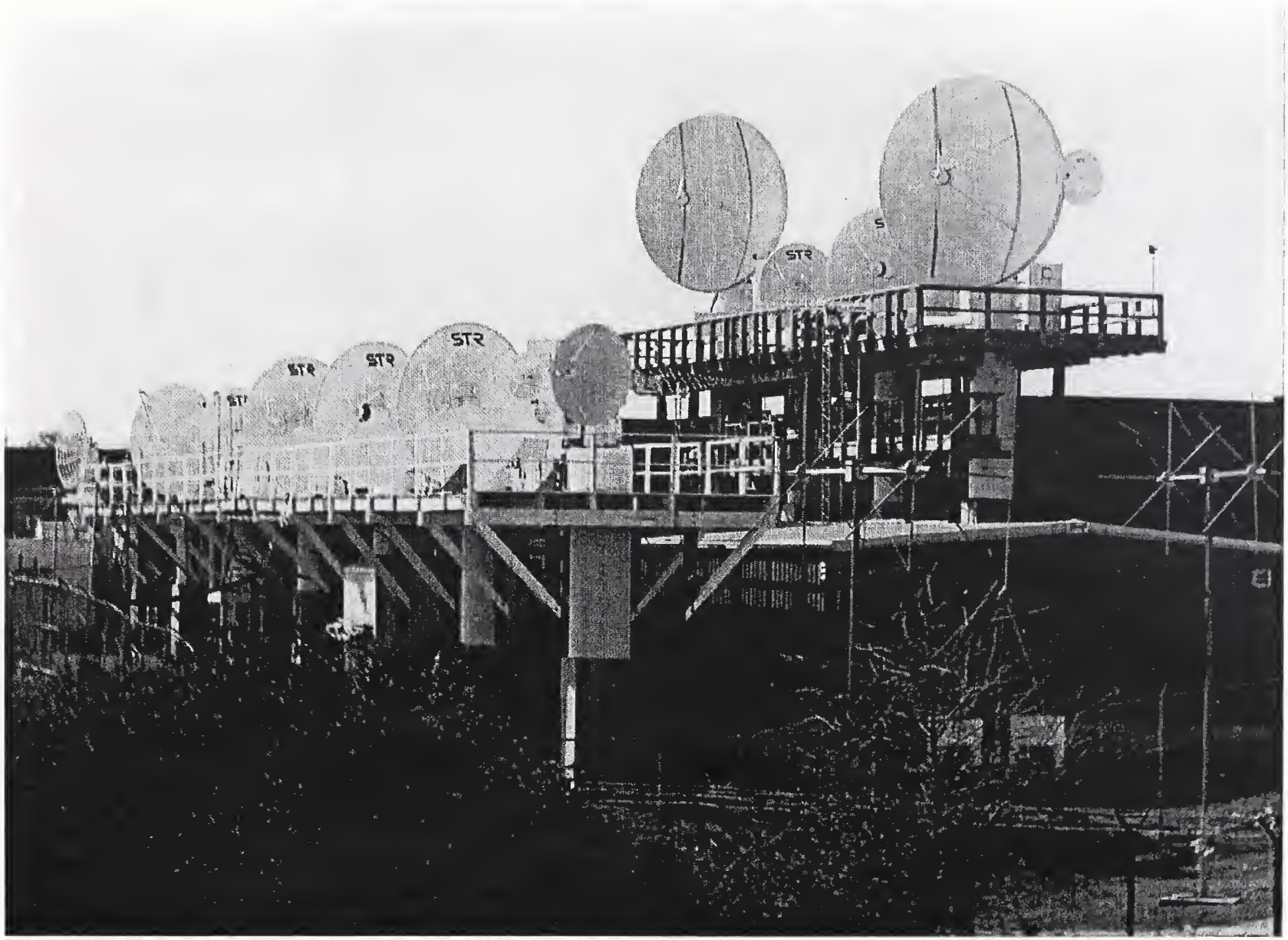

Figure 2: The Atlantic Test Range antenna farm.

uncertainties and should be carefully evaluated and reviewed by range personnel.

4. This document reflects current understanding. It will be *reviewed* periodically and *revised* to incorporate improved methods of uncertainty estimation and to account for changes in measurement methods and/or hardware. This report will be submitted for review during the range certification process [2].

2 Reporting Measurement Uncertainty

A measurement of RCS σ, should be quantified by a statement of uncertainty

$$\sigma = \sigma_0 \pm \Delta\sigma, \tag{1}$$

where σ_0 indicates the best RCS estimate, and $\Delta\sigma > 0$ is a defendable *bound* for the measurement error. Error bounds need not be symmetric, but may be of the form

$$\sigma_0 + \Delta\sigma_+ > \sigma > \sigma_0 - \Delta\sigma_-. \tag{2}$$

For simplicity, we will continue to use eq (1) with $\Delta\sigma = \max(\Delta\sigma_+, \Delta\sigma_-)$.

Uncertainties are also stated logarithmically

$$\Delta\sigma_\pm \text{ (dB)} \equiv \pm 10 \log\left(1 \pm \frac{\Delta\sigma}{\sigma_0}\right). \tag{3}$$

As before, we will often use symmetric bounds. In this case, since $\Delta\sigma_-$ (dB) $\geq \Delta\sigma_+$ (dB),

$$\Delta\sigma \text{ (dB)} \equiv \Delta\sigma_- \text{ (dB)} = -10 \log\left(1 - \frac{\Delta\sigma}{\sigma_0}\right). \tag{4}$$

Unsymmetrical bounds may be given when reporting larger logarithmic uncertainties. For example, if $\Delta\sigma/\sigma_0 = 1$, then $\Delta\sigma_+$ (dB) ≈ 3, while $\Delta\sigma_-$ (dB) $= \infty$. (We assume that $\Delta\sigma/\sigma_0 < 1$, otherwise the logarithmic uncertainty is undefined.)

A sample uncertainty analysis is shown in Table 1. Table 1(a) shows uncertainties related to measurement of the test target; Table 1(b) shows uncertainties associated with the primary calibration target. *The numbers*

(a) TEST TARGET UNCERTAINTIES		estimates [dB]
3.1	Average Illumination	0.7
3.2	Background-Target Interactions	neg.
3.3	Cross Polarization	0.6
3.4	Drift	0.3
3.5	Frequency	0.0
3.6	Integration	0.0
3.7	I-Q Imbalance	n.a.
3.8	Near Field	0.3
3.9	Noise-Background	0.3
3.10	Nonlinearity	0.3
3.11	Range	0.0
3.12	Target Orientation	n.a.
3.13	Reference RCS (4.14)	1.0
3.14	Combined Uncertainty (RSS)	**1.1** **-1.5**

(b) CALIBRATION TARGET UNCERTAINTIES		estimates [dB]
4.1	Average Illumination	0.7
4.2	Background-Target Interactions	neg.
4.3	Cross Polarization	0.0
4.4	Drift	0.3
4.5	Frequency	0.0
4.6	Integration	0.0
4.7	I-Q Imbalance	n.a.
4.8	Near Field	neg.
4.9	Noise-Background	0.5
4.10	Nonlinearity	0.3
4.11	Range	neg.
4.12	Target Orientation	neg.
4.13	Reference RCS	neg.
4.14	Combined Uncertainty (RSS)	1.0

Figure 2: The Atlantic Test Range antenna farm.

to the left of each entry are references to the section of this report[1] *where the corresponding uncertainty is discussed.* Individual sources of uncertainty (called components of uncertainty) are listed in each table. The combined (RSS) estimates of uncertainty are shown as the last element of each table. (We assume that components of uncertainty have been delineated so that they are independent, at least approximately. If strong correlations between components of uncertainty were present, our analysis would have to be modified. Presence of correlations could be indicated by a disagreement between uncertainty estimates and observations.) Uncertainties are reported logarithmically. An uncertainty of "neg." indicates that the effect is *assumed* to be unimportant relative to other uncertainties considered in this report, and no specific value for uncertainty is computed. A computed value is always reported, even if the uncertainty is very small. An entry of "n.a." indicates that this source is not considered a factor in the current evaluation (integration error, for example, is not applicable when the target is stationary).

The entries are an attempt to represent *typical* NAWC-AD uncertainties. Actual uncertainties, however, depend strongly on the measurement configuration. *Again, an uncertainty analysis should be performed for each measurement configuration.* For example, uncertainty tables should be given as a function of signal or for different frequency bands.

The method of uncertainty combination is root sum of squares (RSS). That is, the combined uncertainty $\Delta\sigma$ is calculated as

$$\left(\frac{\Delta\sigma}{\sigma_0}\right)^2 = \sum_i \left(\frac{\Delta\sigma_i}{\sigma_0}\right)^2, \tag{5}$$

where $\Delta\sigma_i$ are the (independent) components of uncertainty. Note that relative (not logarithmic) uncertainty is used in the calculation of eq (5). That is,

$$\frac{\Delta\sigma}{\sigma_0} = 1 - 10^{-\Delta\sigma(dB)/10}. \tag{6}$$

We generally retain 2 decimal places in components of uncertainty in order to avoid accumulation of round-off errors. In fact, calculations were performed to full precision in Table 1, which was created using a spreadsheet program.

In turn, each component of uncertainty may be the combined uncertainty of a separate lower level table. Table 1(b) is an example, which gives uncertainties associated with the standard target calibration. The combined

[1] Sections here generally parallel the sections of NISTIR 5019 [1].

calibration uncertainty (line 4.14) is included in Table 1(a) as a contribution to the test target measurement uncertainty (line 3.13, Reference RCS). Tables 1(a) and 1(b) are a convenient upper level summary of the major features of the analysis. Each component of uncertainty in these tables could be a combined (RSS) estimate from a lower level table of uncertainties, etc.

The term *estimate* is applied subjectively. *Estimates of uncertainty will generally be strongly influenced by practical experience.* This is especially true for uncertainties which depend on the nature of the target, such as those associated with cross-polarization errors. *Loosely speaking, we are 95% confident that the actual error falls within the estimated uncertainty bounds.* When the uncertainty in a parameter has been obtained statistically, we choose a two standard deviation confidence bound as the estimate.

3 Test Target Uncertainties

The radar equation can be expressed as a ratio of test target RCS to calibration target RCS:

$$\frac{\sigma_0}{\sigma_s} = \left(\frac{R}{R_s}\right)^4 \left(\frac{G_s}{G}\right)^2 \left(\frac{f}{f_s}\right)^2 \frac{P_{ts}}{P_t} \frac{P_r}{P_{rs}}, \tag{7}$$

where

$$\begin{aligned} \sigma &= \text{radar cross section [m}^2\text{]}, \\ R &= \text{range (distance) [m]}, \\ G &= \text{antenna gain}, \\ f &= \text{frequency [Hz]}, \\ P_t &= \text{transmitted (delivered) power [W]}, \\ P_r &= \text{received power [W]}. \end{aligned}$$

The subscript s identifies quantities associated with the standard calibration target. For example, we allow the possibility that $G_s/G \neq 1$, as could result from pointing errors.

3.1 Average Illumination

We assume plane-wave illumination. (In practice, there will be some illumination taper for extended targets, see Section 3.8.) Average illumination uncertainties result from

(1) pointing errors,
(2) multipath illumination.

Pointing error. According to Reference [1, eq (9)]

$$\Delta\sigma_p \text{ (dB)} = -40 \log \cos\left(\frac{\pi\theta}{4\theta_0}\right), \tag{8}$$

where $2\theta_0$ is the antenna's 3 dB beamwidth and θ is the worst-case pointing error. This equation assumes that the antenna has a $\cos^2$ pattern and is optimally boresighted. Let $2\theta_0 = 0.7°$ and $\theta = 0.1°$ (see Appendix B).

Estimated uncertainty: $\Delta\sigma_p$ (dB) = 0.44

Multipath illumination error. For dynamic ranges, especially over water, there can be an indirect illumination path which involves specular reflection from the surroundings. This contribution will alter the effective gain depending on the relative phase between the direct and indirect rays. Multipaths that impinge on the target only once are considered here. (Paths that impinge on the target more than once are considered in the section on background-target interactions.) These signals travel along the antenna-surface-target-antenna path, the antenna-target-surface-antenna path, and the antenna-surface-target-surface-antenna path. (The contribution from the antenna-surface-target-surface-antenna path is negligible compared to the other two.)

RCS uncertainty may be crudely estimated using the worst possible variation in effective gain

$$\Delta\sigma_m \text{ (dB)} = 20 \log_{10}\left(\frac{1+x}{1-x}\right) \tag{9}$$

$$x = 2\rho 10^{-|\Delta G|/20}, \tag{10}$$

where ρ is a reflection coefficient. ΔG is difference in the gain along the direct path and the gain along the indirect path, which are separated by $2\theta_e$ (twice the elevation angle; see Appendix C). When x is small

$$\Delta\sigma_m \text{ (dB)} \approx 17.4x. \tag{11}$$

For $\rho = 0.5$ and $\Delta G = -30$ dB

$$\Delta\sigma_m \text{ (dB)} \approx 0.55 \text{ dB}. \tag{12}$$

Contributions $\Delta\sigma_p$ and $\Delta\sigma_m$ may be combined RSS to give the combined uncertainty due to uncertainties in illumination.

Estimated uncertainty: $\Delta\sigma$ (dB) = 0.72

3.2 Background-Target Interactions

Background-target interaction is strongest where the target and mounting mechanism are closely coupled due to physical proximity. Under such conditions time gating is of limited value. When coupling is between distant targets, we generally do not expect background-target uncertainties to be significant. In general, this condition holds true for dynamic RCS ranges.

For airborne targets the background-target interactions consist of multipath interference between the aircraft and the ocean surface. Here signal paths that impinge on the target more than once are considered. (Contributions from paths that include the target only once are examined in the section treating average illumination.)

Estimated uncertainty: negligible.

3.3 Cross Polarization

A significant measurement error can result if the radar system does not have perfect polarization isolation. In Reference [1], an example is given with a "moderately" depolarizing target for which the cross polarization uncertainty is [1, eq (13)]

$$\Delta\sigma \text{ (dB)} = -20\log(1 - 2 \times 10^{-\epsilon_p/20}), \tag{13}$$

where ϵ_p is the antenna polarization isolation in decibels. (This model assumes that the elements of the scattering matrix are equal.) In system 8 the antenna polarization isolation ϵ_p is approximately 29 dB (see Appendix D).

Estimated uncertainty: $\Delta\sigma$ (dB) = 0.64

3.4 Drift

The uncertainty attributable to drift in the measurement system can be determined by making measurements on a fixed target over an extended time. Drift data were collected over a 3 h period. This period is based on the duration of a typical test. For the period indicated, the estimated uncertainty is

0.30 dB. Further details and dataset characteristics are included in Appendix E.

Estimated uncertainty: $\Delta\sigma$ (dB) = 0.30

3.5 Frequency

The uncertainty in RCS due to uncertainty in frequency is given by Reference [1, eq (14)]

$$\Delta\sigma \text{ (dB)} = -20\log(1 - \Delta f/f), \tag{14}$$

where Δf is the effective system bandwidth, and f is the center frequency. For the measurement system under consideration $f = 9.2$ GHz and $\Delta f = 10$ MHz.

Equation (14) assumes that test target RCS, calibration target RCS, and system gain are not strong functions of frequency. An example with strong frequency dependence is given in [1, Appendix C].

Estimated uncertainty: $\Delta\sigma$ (dB) = 0.01

3.6 Integration

Integration uncertainty is due to *target motion* during the time of a *single pulse*. The largest uncertainty in position ΔR during a radar pulse of duration τ will be due to motion of the target along the line of sight from the radar to the target. For $\tau = 1$ μs, $v = 130$ m/s and $\Delta R = v\tau = 1.30 \times 10^{-4}$ m. This uncertainty in position gives the upper bound of the uncertainty in RCS as [5, Appendix H]

$$\Delta\sigma \text{ (dB)} = -40\log(1 - \Delta R/R_t) \tag{15}$$

Estimated uncertainty: $\Delta\sigma$ (dB) = 0.

3.7 I-Q Imbalance

In the noncoherent RCS measurement system under consideration I-Q imbalance is not applicable.

3.8 Near Field

The near field uncertainty in RCS is due to nonuniform illumination across the target. The radar equation (7), assumes that the target is illuminated by a plane wave. Large aircraft targets on the NAWC-AD radar measurement range may not meet this condition. The incident field will have some taper across the length of the aircraft, especially when it is broadside to the radar. *A simple, but crude estimate of uncertainty is the maximum variation in signal over the target.*

A target of length $2r = 2 \times 15.5$ m at a distance $R = 11$ km subtends an angle $\theta_v = \tan^{-1}(r/R) \approx 0.08°$. The amplitude taper in the radiation pattern across this length is obtained from the antenna pattern (see Appendix A); the gain reduction at θ_v is bounded by ΔG_{Az}, $\Delta G_{El} < 0.3$ dB. (Alternatively, eq (8) yields $\Delta G = 0.28$ dB.)

Estimated uncertainty: $\Delta\sigma$ (dB) = 0.3

3.9 Noise-Background

System noise will contribute to measurement errors. For signal S and noise-background N, the RCS uncertainty is calculated as

$$\Delta\sigma \text{ (dB)} = -20 \log \left(1 - 10^{-\epsilon_n/20}\right), \tag{16}$$

where $\epsilon_n = 20 \log (S/N)$. We typically include quantization effects in this category (see Appendix F for details), and we use the worst-case signal level to determine the uncertainty. Assume $\epsilon = 30$ dB (see Appendix F).

Estimated uncertainty: $\Delta\sigma$ (dB) = 0.3

3.10 Nonlinearity

Receiver nonlinearity is measured as follows: a synthesizer is used to inject a constant calibration signal into the receiver. The precision attenuators are integrated as a permanent component of the receiver system. The output of the receiver is measured as the attenuators step through their range of values. Software corrects for receiver nonlinearity, leaving only a residual attenuator uncertainty. Attenuator uncertainties were reported by the manufacturer and are NIST traceable. We use the largest attenuator uncertainty, which occurs at 40 dB.

Estimated uncertainty: $\Delta\sigma$ (dB) = 0.32

3.11 Range

The uncertainty in RCS due to uncertainty in the range R is given by Reference [1, eq (18)]

$$\Delta\sigma \text{ (dB)} = -40 \log(1 - \Delta R/R_t) \tag{17}$$

with $\Delta R = \Delta R_t + \Delta R_{tr}$, where ΔR_t is the change in range due to target motion during data transmission (data latency effect), and ΔR_{tr} is the uncertainty in the range tracker. For R_t = 11 km, ΔR_{tr} = 2.74 m, and $\Delta R_t = v_t t_{dl} = (128.7)(0.126) \approx 16$ m. Hence, $\Delta R \approx 19$ m.

Estimated uncertainty: $\Delta\sigma$ (dB) = 0.03.

3.12 Target Orientation

Since we are primarily interested in the levels of peak and sidelobes, and not in their exact angular locations, we consider this uncertainty to be not applicable.

Estimated uncertainty: not applicable.

3.13 Reference RCS

This result is the combined uncertainty of the calibration target measurement (see 4.14).

Estimated uncertainty: $\Delta\sigma$ (dB) = 1.0

3.14 Combined Uncertainty (RSS)

The RSS of the uncertainties 3.1 through 3.13 gives combined uncertainties of $\Delta\sigma_-$ (dB) = 1.5 and $\Delta\sigma_+$ (dB) = 1.1. See eq (3). [Components of uncertainty are summarized by section number in Table 1(a).]

4 Calibration Target Uncertainties

The following series of calculations define the uncertainty associated with the primary calibration target, which is a sphere.

The calibration sphere is tethered to a helium-filled weather balloon and released. Tracking radars at the NAWCAD acquire and track the sphere while RCS measurements are made. The sphere is typically tracked from 8 to 30 km, which is the typical range over which measurements on aircraft are made.

The sphere with $r \approx 30$ cm has a radar cross section of -11.4 dB re 1 m^2 (dBsm). The balloon is a seamless, 3.50×10^{-5} kg meteorological balloon made of rubber and chloroprene; the tether is a thin cloth tape 25 m long and 0.8 cm wide.

The combined calibration uncertainty must be supported by observation. In this study the observed variation in the power received from the calibration sphere sometimes exceeds the uncertainty estimate given in Section 4.14 below. Further analysis is necessary to explain and correct this discrepancy; one possibility is that correlations between the uncertainty components have not been properly taken into account.

4.1 Average Illumination

We can assume far-field illumination if the location of the target satisfies the usual $2D^2/\lambda$ criterion. For spheres used at the ATR this condition is easily satisfied. The RCS uncertainty contribution, in this case, consists of multipath and pointing errors, and is treated as in Section 3.1.

Estimated uncertainty: $\Delta\sigma$ (dB) $= 0.72$.

4.2 Background-Target Interactions

This contribution to RCS uncertainty comes mainly from multiple scattering interactions among the calibration sphere, the balloon, and the string. We estimate this uncertainty to be negligible.

Estimated uncertainty: negligible.

4.3 Cross Polarization

The sphere is not a depolarizing target. For such targets Reference [1, eq. 4.3] shows that the uncertainty may be estimated as

$$\Delta\sigma(\text{dB}) = -20\log(1 - 10^{-\epsilon_p/10}). \tag{18}$$

The antenna polarization isolation was measured to be $\epsilon_p = 29$ dB (see Appendix D).

Estimated uncertainty: $\Delta\sigma$ (dB) = 0.01.

4.4 Drift

The uncertainty due to drift is the same as in Section 3.4 (see Appendix E).

Estimated uncertainty: $\Delta\sigma$ (dB) = 0.3.

4.5 Frequency

The uncertainty due to the finite bandwidth of the system is the same as in Section 3.5.

Estimated uncertainty: $\Delta\sigma$ (dB) = 0.01.

4.6 Integration

Integration uncertainty is due to the motion of the calibration target during the time of a *single pulse*. The uncertainty is maximum when the target is moving along the line of sight between the target and the RCS system during a radar pulse of length τ s. For our RCS system, $\tau = 1$ μs, $v_s = 25.0$ m/s, and $\Delta R = v_s\tau = 2.5 \times 10^{-5}$ (see [3], Appendix H). The uncertainty in RCS is given by

$$\Delta\sigma \text{ (dB)} = -40\log(1 - \Delta R/R_s) \tag{19}$$

Estimated uncertainty: $\Delta\sigma$ (dB) = 0.

4.7 I-Q Imbalance

In the incoherent RCS systems examined in this report for I-Q imbalance detection is not applicable.

Estimated uncertainty: not applicable.

4.8 Near Field

The calibration sphere is in the far field of the antenna; therefore, the amplitude taper across the sphere is negligible (see Section 3.8). The corresponding uncertainty in RCS is also negligible.

Estimated uncertainty: negligible.

4.9 Noise-Background

For a signal-to-noise ratio of ϵ (dB), the uncertainty in RCS is obtained from

$$\Delta\sigma \text{ (dB)} = -20\log(1 - 10^{-\epsilon/20}). \tag{20}$$

Since S/N depends on the range R in a dynamic measurement, we control the noise uncertainty by accepting measurements with $\epsilon > 20\log(S/N) = 25$ dB, since the RCS of the balloon is 25 dB below the RCS of the calibration sphere. This was determined with the coherent imaging radar system at the NAWCAD (see Appendix F).

Estimated uncertainty: $\Delta\sigma$ (dB) = 0.5.

4.10 Nonlinearity

The uncertainty due to nonlinearity was described in Section 3.10.

Estimated uncertainty: $\Delta\sigma$ (dB) = 0.32.

4.11 Range

The uncertainty in RCS due to uncertainty in the range R is given by

$$\Delta\sigma = -40\log(1 - \Delta R/R_s), \tag{21}$$

where $R_s = 11$ km, and $\Delta R = \Delta R_s + \Delta R_{tr}$, where ΔR_s is the change in range due to target motion during data transmission (data latency effect), and ΔR_{tr} is the uncertainty in range tracking. For $\Delta R_{tr} = 2.7$ m and $\Delta R_s = v_s t_{dl} \approx (25.0)(0.13) \approx 3.3$ m, $\Delta R = 5.9$ m.

Estimated uncertainty: $\Delta\sigma$ (dB) = 0.01.

4.12 Target Orientation

The calibration sphere is assumed symmetric, so change in target orientation will introduce negligible uncertainty in RCS. The uncertainty introduced by any deviation from the ideal sphere is included in the Section 4.13 below.

Estimated uncertainty: negligible.

4.13 Reference RCS

The sphere is one of the few objects whose RCS can be calculated to arbitrary accuracy; however, deviations from ideal spherical shape, finite and variable surface conductivity, and surface roughness (local irregularity) all contribute to calibration uncertainty. We need to study the effects of these perturbations on the predicted RCS of a sphere. For now we assume that this uncertainty component is negligible, but further study is recommended (see Section 5).

4.14 Combined Uncertainty (RSS)

The RSS of the uncertainties in 4.1 through 4.13 gives an combined RCS uncertainty of 1.0 dB. [Components of uncertainty are summarized by section number in Table 1(b).]

5 Tasks for the Future

This document summarizes the current uncertainty analysis used at NAWC-AD. Further work is needed in a number of areas to improve uncertainty estimation and measurement procedures. For example, the combined uncertainty in sphere calibration (see point 8 below) does not support the large observed variation in the measured data.

Here are some topics for future consideration:

1. *Illumination.* The treatment of average illumination and near-field uncertainties needs to be strengthened. Perhaps Average Illumination and Near Field should be combined in a single subsection: Illumination. The effect of phase error should also be examined.

   The complete scattering-matrix theory could be considered to see if a more satisfactory treatment of illumination uncertainty is practical.

2. *Documentation of Best Estimate Trajectory (BET).* The BET analysis is routinely conducted by a dedicated staff of mathematicians. Currently this procedure is not documented in a manner that can be readily referenced. A short document explaining the mathematical techniques used, together with sample data analysis and results, should be prepared and *reviewed for technical soundness* in the near future.

3. *Long term stability.* Measurement uncertainty (Section 4) depends on the stability of system parameters over the time interval between the primary calibration and the measurement on the target under test. This long term *drift* needs to be characterized.

4. *Secondary check standard.* A secondary check standard should be used to monitor drift during measurements.

5. *Sea state.* Further observational study should be planned to determine how strongly sea state affects aircraft RCS through multipath interference. Is there a better way to quantify the condition of the ocean surface?

6. *Polarization.* Actual polarimetric data from aircraft targets should be used to validate our estimates of cross-polarization uncertainty. The practicality of a fully polarimetric calibration should be examined [4], [5], [6].

7. *Frequency.* The sensitivity to frequency of aircraft targets and radar systems should be considered in our estimates of frequency uncertainty.

8. *Sphere calibration.* Variations seen in RCS data for calibration spheres sometimes considerably exceeds the uncertainty estimate in Section 4.14. This variation may be partly due to tracking inaccuracies. The parameters associated with tracking inaccuracies need to be re-evaluated.

Other sources of uncertainty are not now understood. Hence, the uncertainty analysis of the sphere calibration needs to be supported with further study. For example, calibration with a sphere must be consistent with measurements made on different size spheres (consistency checks). In addition, data analysis techniques should be re-examined. For example, instead of averages, perhaps the peak returns should be used [3].

9. *Sphere-balloon interaction.* The illumination of the balloon and string supporting the dynamic sphere contributes to the background-target interaction. This needs closer theoretical examination and must be verified by measurements.

10. *Calibration sphere imperfections.* Estimates of uncertainty due to the finite conductivity of the sphere should be developed. Similarly, uncertainties due to coatings on the sphere should be researched, and shape effects such as deviations from sphericity need more detailed analysis.

11. *Cross polarization.* Procedures for determining cross polarization should be reviewed. The physical alignment and orientation of the radiating horn used to determine polarization isolation should be independently monitored to detect possible misalignment of the vertical polarization axis. Long term records of cross-polarization checks should be kept.

A Appendix NAWC-AD radar system parameters and operating conditions

The operating parameters assumed to hold in this report are:

1. The RCS measurement system 8 (I band) is *noncoherent.*
2. Measurement configuration is monostatic RCS
3. Targets are dynamic and airborne
4. Operating frequency is $f = 9.2$ GHz
5. Distance of unknown target to RCS measurement system is $R \approx 11$ km

6. Test target velocity is $v \approx 130$ m/s

7. Elevation angle of test target is $\theta_e = 5°$

8. Calibration target distance to RCS measurement system $R_s \approx R$

Typical operating parameters are:

Transmitter power: 100 kW peak

Antenna gain: 44 dB for antenna 8, a 3 m paraboloid reflector

Pulse width: 1 μs

Effective receiver bandwidth: 1 MHz

Pulse repetition frequency: 640 Hz

The available operating frequencies and the corresponding bands are:

1.2 GHz ±5 MHz (D band)
2.9 GHz ±5 MHz (E band)
5.5 GHz ±5 MHz (G band)
6.5 GHz ±5 MHz (H band)
9.2 GHz ±5 MHz (I band)
15.2 GHz ±5 MHz (J band)
34.7 GHz ±5 MHz (K band)

A typical antenna pattern considered in this study (obtained from the manufacturer during acceptance testing) is shown in the Figure 3:

B Appendix Average Illumination

The unknown target's position is determined with a tracking radar system. Time, space, position information (TSPI) from the tracking radar is sent to the RCS measurement system's antenna positioner, which aims the antenna to illuminate the unknown target.

The average illumination uncertainty is maximum when the unknown target is moving transversely to the line of sight of the antenna. This determines our uncertainty estimate.

Parameters affecting positioner uncertainty include: nonorthogonality (ϵ_{no}), gearing backlash (ϵ_{gb}), static error (ϵ_{st}), velocity dependent position error

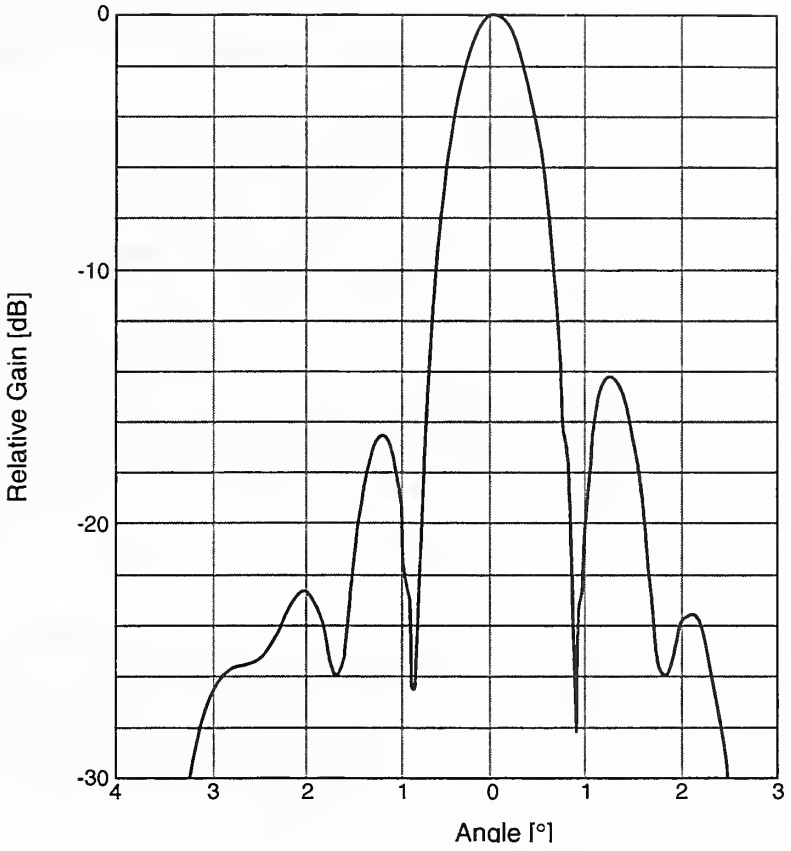

Figure 3: ATR 9.2 GHz antenna pattern (vertical polarization).

(ϵ_{vl}), tracking radar uncertainty (ϵ_{tr}), dynamic error (ϵ_{dy}), and data latency (t_{dl}).

Manufacturer's positioner specifications indicate the following: $\epsilon_{no} = 0.02°$, $\epsilon_{gb} = 0.05°$, $\epsilon_{st} = 0.05°$, $\epsilon_{vl} = 0.003°/°/s$ and $\epsilon_{tr} = 0.014°$. These tolerances are currently accepted without verification.

The nonorthogonality uncertainty arises because the elevation and azimuth axes of the positioner are not perfectly orthogonal. Gearing backlash uncertainty is the amount of error that could result from mechanical backlash of the positioner gear drive. The static and dynamic errors are a measure of how the positioner and its electronic controller interact. The static error

is the maximum angular error observed while the positioner is at rest. The dynamic error is a measure of how accurately the positioner can be pointed during a dynamic measurement. Worst case dynamic error is calculated using maximum (transverse) flight paths.

Tracking radar angular errors are determined monthly at the ATR as part of a formal Range System Accuracy Evaluation (RSAE), and the results are reported to the Range Commanders Council biannually. Several methods using different range assets are available to determine system accuracy. In one of the methods we obtain a *best estimate trajectory (BET)* using a Kalman filter on the various TSPI data received from a tethered sphere. The TSPI sources available for these measurements include 3 I-band tracking radars, 4 theodolites, and 2 lasers. Another commonly used method to determine system accuracy compares GPS TSPI data from an airplane with TSPI data from other sources. In both methods, the tracking errors are quantified statistically; 2 standard deviation confidence bounds are used. These analyses are routinely carried out by a permanent staff of mathematicians (see Section 5).

Data latency is the time it takes data to be transmitted from the tracking radar to the antenna positioner. The estimated angular error is then obtained using the positioner angular rates corresponding to a transverse flight path. Data latency is measured experimentally by time-tagging TSPI data at the tracking radar and comparing the tag with the time at which the data reaches the multiple antenna positioning system (MAPS).

The above uncertainties are combined using RSS to yield the total positioner uncertainty.

B.1 Primary calibration target (sphere)

The positioner dynamic error ϵ_{dy} is given by

$$\epsilon_{dy} = \frac{180}{\pi}\epsilon_{vl}\omega = 0.000\ 38^\circ, \tag{22}$$

where ϵ_{vl} is the velocity dependent error in position, and

$$\omega = \frac{v_s}{R_s}, \tag{23}$$

where ω [rad/s] is the positioner angular velocity, $v_s \approx 25$ m/s is the velocity of the sphere, and

$$\epsilon_{dl} = \frac{180}{\pi}t_{dl}\omega = 0.016^\circ \tag{24}$$

is the error due to data latency. In eq (24) $t_{dl} = 0.13$ s, which was obtained experimentally as outlined above.

Combining all of the above uncertainty components in a RSS sum yields,

$$\epsilon_{rss} = \sqrt{\epsilon_{no}^2 + \epsilon_{gb}^2 + \epsilon_{st}^2 + \epsilon_{tr}^2 + \epsilon_{dy}^2 + \epsilon_{dl}^2} = 0.08°. \quad (25)$$

From the antenna pattern data, the one-way reduction in gain at angle ϵ_{rss} from boresight is $\Delta G = 0.28$ dB. The two-way gain reduction gives the average illumination error for the sphere calibration target.

B.2 Plane target

The average illumination uncertainty is obtained as for the sphere (see above). The velocity of the plane is assumed to be $v \approx 130$ m/s; hence, $\epsilon_{dl} = 0.088°$, and $\epsilon_{rss} = 0.012°$. From the antenna pattern we obtain an uncertainty of 0.62 dB.

C Appendix Near-Field Effects (Average Illumination)

Multipath effects can be calculated from the flat earth model [7] shown in Figure 4, where γ is the reflected ray grazing angle, θ_e is the elevation angle of the target, h is the height of RCS system's antenna above the earth's surface.

When $h/d << 1$, the multipath reflection point on the surface is located at an angle θ from the direct path ray to the target, where

$$\theta = \theta_e + \gamma \approx 2\theta_e = 10°. \quad (26)$$

From the antenna pattern data, the antenna gain is -30 dB down at 10° from the peak. This attenuated multipath signal is modified by the surface reflection coefficient $\rho = \rho_0 \rho_s$, where ρ_0 is the reflection coefficient of the surface, $0 \leq \rho_s \leq 1$ (1 for a smooth surface) represents the specular component of the wave due to surface roughness. $\rho_0 = 1$ is the worst case, which holds for horizontally polarized radiation. The surface roughness can change depending on the weather conditions; conservatively, we can choose $\rho_s = 0.5$ to characterize the state of the water surface (independent of time). These values yield $\rho = 0.5$. The uncertainty in RCS due to multipath reflection effects can now be calculated as indicated in Section 3.1.

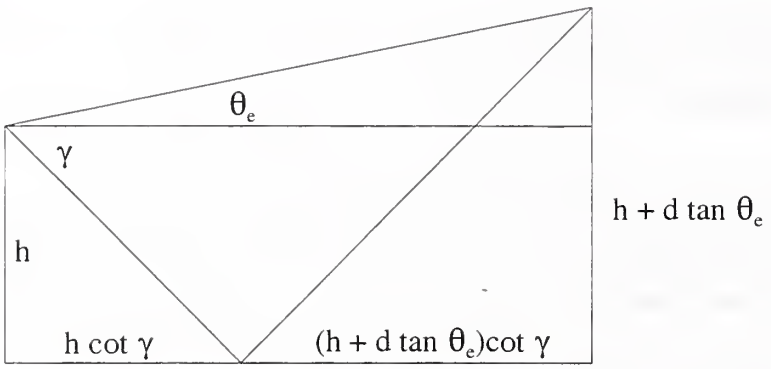

Figure 4: Direct and indirect illumination for a flat earth model.

D Appendix Cross Polarization

We determine the polarization isolation of the RCS measurement system as follows:

We use a signal generator, a linearly polarized horn antenna, the RCS receiving antenna and a spectrum analyzer. The receiving antenna has vertical and horizontal polarization ports that operate simultaneously; the horn antenna has a cross polarization isolation greater than 40 dB. The radiating horn, fed by the signal generator, is positioned in the far-field of the receiving antenna, and the spectrum analyzer is connected to an output port of the receiving antenna. The horn antenna is rotated until the maximum amplitude response to a vertically transmitted signal is observed on the spectrum analyzer. The responses at both the vertical port and the cross-polarized port are recorded with the spectrum analyzer. The procedure is repeated using a horizontally transmitted signal. In this manner we obtain the receiving amplitudes R_{vv}, R_{vh}, R_{hv}, and R_{hh}, where the first subscript identifies the polarization of the receiving port and the second subscript identifies the polarization of the transmitting port. *In the above procedure we assume that the receiving antenna has been properly aligned during installation and remains aligned* (see Section 5).

We can now calculate the polarization isolations ϵ_p, where $p = h$ or v [5].

Thus, in decibels,

$$\epsilon_h = R_{hv} - R_{hh}, \tag{27}$$

$$\epsilon_v = R_{vh} - R_{vv}, \tag{28}$$

and the gain imbalance ρ of the two polarization channels can be obtained from

$$\rho = R_{vv} - R_{hh}. \tag{29}$$

We define the cross-polarization ratio as $\epsilon_p = \min(\epsilon_{hv},\ \epsilon_{vh})$, which is used to determine the cross-polarization uncertainty.

E Appendix Drift

E.1 Short-term drift

By *short-term* drift we mean the drift in the received signal observed during a time interval equal to or less than the time needed to complete a calibration or to measure a target.

The drift is measured by operating the system in a typical measurement mode with modifications. The transmitted RF is coupled from the waveguide to the receiver, which is located inside the operations building. The system is operated at a pulse repetition frequency of 640 Hz, 1 μs pulse width, at the nominal rated power. Every pulse is received, digitized, processed, and recorded during the test, and a reduced dataset consisting of one sample per second is created. Statistics are then performed on the dataset, and the short term drift is quantified. The variation from pulse to pulse over the measurement period appeared to be random. Since processed RCS measurements are presented as a probability function, the uncertainty due to drift was calculated to be twice the standard deviation of the sampled data set.

Data set characteristics:

Duration: 3 h
Size: 10 800 samples
Mean: 7.86 dB re 1 mW
Standard Deviation: 0.156 dB re 1 mW

E.2 Long-term drift

By *long-term* drift we mean the drift in the received signal observed between calibration and measurements. Such drift data have diagnostic value, since large variation in the received signals need to be explained in terms of environmental conditions and system changes.

Long-term drift is not now being measured. Methods to measure long-term drift are under investigation. A permanent, fixed calibration target that can be used for this study is currently being installed and characterized.

For both short- and long-term future drift measurements, we plan to operate the RCS system with no modifications to make measurements easier to perform, with only little lost range time. This will result in more realistic drift assessments.

F Appendix Noise-Background

F.1 Noise

The S/N ratio is determined by the following method: the reflected energy is measured, using the RCS data collection system, as a calibration sphere is launched and carried down range by the wind. The same RCS data collection system is then used to measure the noise present in each range bin, in the absence of the calibration sphere. These two measurements determine the S/N ratio for the calibration sphere. The S/N ratio of the unknown target is then calculated by substituting the expected return signal from the target for S, and recalculating S/N using the previously measured noise N. For the purposes of this analysis, the unknown target is assumed to have a radar cross section of 0 dB re 1 m^2.

In Figure 5 we show the power returned from a sphere with $r = 30$ cm during a pre-flight calibration measurement; the noise received is also shown.

F.2 Background—The RCS of the balloon

The signal received from the balloon is part of the *background*, which is the signal received when no target is present. A balloon was with no sphere

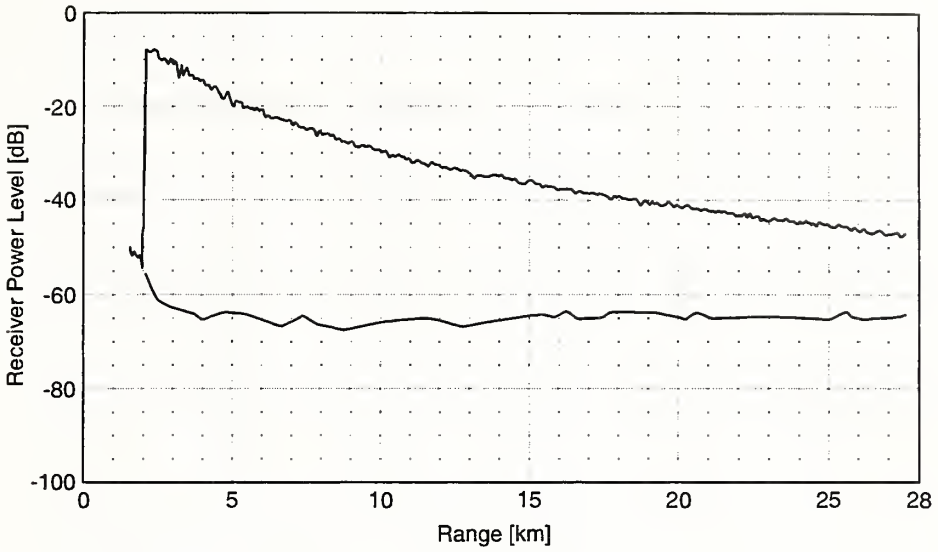

Figure 5: The received power level from a 12 in sphere as a function of range. The received noise power is also shown (lower line).

attached was measured directley and its RCS was compared to the RCS of a sphere-balloon combination. The RCS of the balloon by itself was about 26 dB below that of the sphere-balloon combination. Figure 6 shows the stepped frequency image of the sphere-balloon combination. As expected, the image of the balloon is about 26 dB below the image of the sphere.

References

[1] R. C. Wittmann, M. H. Francis, L. A. Muth, and R. L. Lewis, *Proposed uncertainty analysis for RCS measurements*, National Institute of Standards and Technology NISTIR 5019, Jan. 1994.

[2] L. A. Muth, R. C. Wittmann, B. M. Kent, Measurement assurance and certification of radar cross section measurements, Proc. Natl. Conf. Stand. Labs., Atlanta, GA, pp. 555–566, 27–31 July 1997.

[3] L. A. Muth, R. C. Wittmann, R. L. Lewis, and R. J. Jost, *A Review of Government RCS Ranges*, National Institute of Standards and Technol-

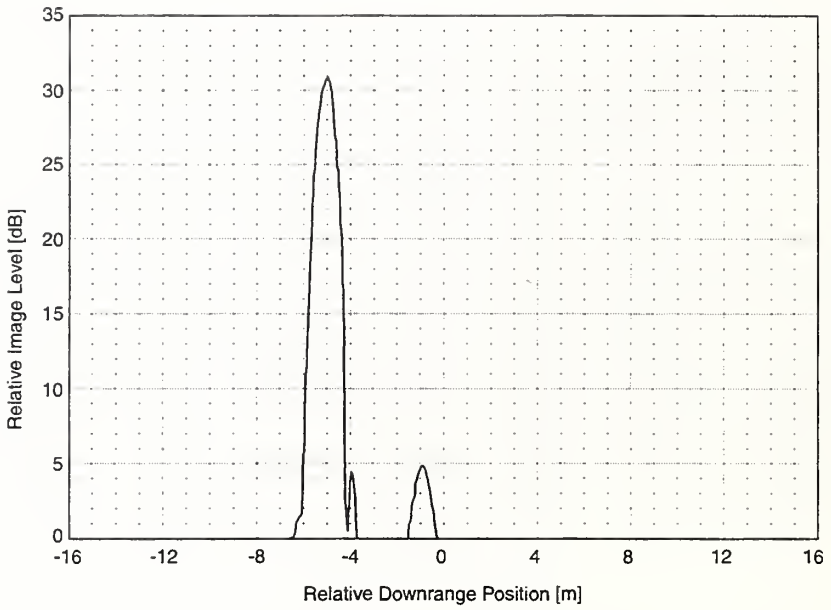

Figure 6: A downrange image of the sphere (large peak) and of the supporting balloon (small peak). The sphere is about 4.8 km from the radar.

ogy, Report to Sponsor, Report Number: 813-123-95, Boulder, CO, Oct. 1995.

[4] R. L. Lewis, L. A. Muth, and R. C. Wittmann, *Polarimetric calibration of reciprocal-antenna radars*, National Institute of Standards and Technology NISTIR 5033, March 1995.

[5] L. A. Muth, R. L. Lewis, and R. C. Wittmann, *Polarimetric calibration of reciprocal-antenna radars*, AMTA Proceedings, pp. 3–8, Williamsburg, VA, 1995.

[6] L. A. Muth, R. C. Wittmann, and W. Parnell, *Polarimetric calibration of nonreciprocal radar systems*, AMTA Proceedings, pp. 389–393, Seattle, WA, 1996.

[7] L. Blake, *Radar Range Performance Analysis*, pp. 249–253, Artech House, Inc., MA, 1986.